Available online at www.sciencedirect.com
SCIENCE DIRECT®
Vision Research 45 (2005) 1385–1398
Vision Research
www.elsevier.com/locate/visres

# Spatial interference among moving targets

Peter J. Bex *, Steven C. Dakin

*Institute of Ophthalmology, University College London, 11-43 Bath Street, London EC1V 9EL, UK*

Received 5 August 2004; received in revised form 18 November 2004

**Abstract**

Peripheral vision for static form is limited both by reduced spatial acuity and by interference among adjacent features ('crowding'). However, the visibility of acuity-corrected image motion is relatively constant across the visual field. We measured whether spatial interference among nearby moving elements is similarly invariant of retinal eccentricity and assessed if *motion integration* could account for any observed sensitivity loss. We report that sensitivity to the direction of motion of a central target—highly visible in isolation—was strongly impaired by four drifting flanking elements. The extent of spatial interference increased with eccentricity. Random-direction flanks and flanks whose directions formed global patterns of rotation or expansion were more disruptive than flanks forming global patterns of translation, regardless of the relative direction of the target element. Spatial interference was low-pass tuned for spatial frequency and broadly tuned for temporal frequency. We show that these results challenge the generality of models of spatial interference that are based on retinal image quality, masking, confusions between target and flanks, attentional resolution limits or (simple) "averaging" of element parameters. Instead, the results suggest that spatial interference is a consequence of the integration of *meaningful* image structure within large receptive fields. The underlying connectivity of this integration favours low spatial frequency structure but is broadly tuned for speed.


*Keywords:* Spatial interference; Crowding; Acuity; Motion; Optic flow

## 1. Introduction

Convergent electrophysiological (Hubel & Wiesel, 1968; Schiller, Finlay, & Volman, 1976; Wurtz, 1969) and behavioural (Anderson & Burr, 1987) studies have established that the classical receptive fields of early visual mechanisms are relatively small and selective for stimulus attributes such as spatial frequency, orientation and direction of motion. In order to derive functional information about large objects and their movements, such local representations must be integrated across the visual field. While pooling is therefore necessary for the perception of global structure, many studies of spatial form discrimination have shown that information about component structure can be degraded in the process of image integration. For example, alphanumeric characters that are reliably identified in isolation can no longer be identified when they are closely surrounded by other optotypes (Bouma, 1970; Townsend, Taylor, & Brown, 1971) or contours (Flom, Weymouth, & Kahneman, 1963). This effect is known as *spatial interference*, *crowding*, or *local contour interaction*. Similarly, discrimination thresholds for the contrast, spatial frequency and orientation of a target grating are elevated by nearby flanking gratings (He, Cavanagh, & Intriligator, 1996; Parkes, Lund, Angelucci, Solomon, & Morgan, 2001; Wilkinson, Wilson, & Ellemberg, 1997). However, crowded elements that cannot be individually identified can nevertheless contribute to the estimate of the mean orientation of the ensemble (Parkes et al., 2001; Wilkinson et al., 1997) and can still generate local, orientation-specific after-effects (He et al., 1996).

* Corresponding author.
*E-mail address:* p.bex@ucl.ac.uk (P.J. Bex).

0042-6989/$ - see front matter © 2005 Elsevier Ltd. All rights reserved.
doi:10.1016/j.visres.2004.12.001

Explanations of crowding have been based on factors that limit resolution at several stages of visual processing. Visual acuity can be reduced under crowded conditions by interactions in the physics of the target and flanking stimuli in the retinal image, such as the point spread function (Liu & Arditi, 2000) or masking by the spatial frequency components they share (Hess, Dakin, & Kapoor, 2000a). However, crowding also occurs between target and flank stimuli that are presented to opposite eyes (Flom et al., 1963; Tripathy & Levi, 1999), implicating a cortical locus for at least some part of spatial interference. Crowding effects are maximal when the spatial (Kooi, Toet, Tripathy, & Levi, 1994; Nazir, 1992), spatial frequency (Andreissen & Bouma, 1976; Chung, Levi, & Legge, 2001; Hess et al., 2000a; Kooi et al., 1994) or orientation (Levi, Klein, & Hariharan, 2002) structure of the target and flanking stimuli are similar. Thus spatial interference is greater among channels that are similarly-tuned for contrast polarity, spatial frequency or orientation than across differently-tuned channels. Tuning properties for foveal crowding are similar to those reported for masking (Polat & Sagi, 1993; Wilson, McFarlane, & Phillips, 1983; Zenger & Sagi, 1996) and consequently some authors have argued that crowding in central vision can be considered a masking phenomenon (Chung et al., 2001; Levi, Hariharan, & Klein, 2002).

While masking might account for crowding in foveal vision, crowding effects in peripheral visual field are not consistent with this explanation and require a different model. In the periphery, crowding effects can be roughly equal for targets and flankers that are of either the same or opposite contrast polarity (Hess, Dakin, Kapoor, & Tewfik, 2000b) although this can depend on eccentricity and location in the visual field (Kooi et al., 1994). The extent of spatial interference does not scale with the spatial frequency of the target as it does on fovea (Chung et al., 2001; Levi, Hariharan, et al., 2002) or with target size (Tripathy & Cavanagh, 2002). These findings rule out masking effects, which scale with spatial frequency in both fovea and periphery (Polat & Sagi, 1993). Instead, the results of peripheral crowding studies implicate a non-selective spatial pooling region of relatively fixed size that may correspond to the spatial resolution of visual attention (He et al., 1996; Intriligator & Cavanagh, 2001; Tripathy & Cavanagh, 2002), the integration stage of later visual processes (Chung et al., 2001) or the region over which grouping and segmentation processes combine texture (Parkes et al., 2001; Wilkinson et al., 1997).

We have recently shown that while acuity falls for moving alphanumeric targets, the spatial extent over which moving elements crowd one another spatial interference is not significantly affected by motion of speeds up to 84 deg/s (Bex, Dakin, & Simmers, 2003). Although resolution for static spatial form rapidly declines in peripheral visual field (Millidot, 1966), sensitivity to temporal modulation (motion and flicker) is relatively invariant across the visual field for detection (McKee & Nakayama, 1984; Wright & Johnston, 1983) and discrimination (McKee & Nakayama, 1984; Waugh & Hess, 1994) tasks, as long as the size and/or contrast of the stimuli is adjusted to compensate for spatial acuity changes. In the case of flicker fusion (the lowest flicker rate that appears steady), sensitivity increases somewhat with eccentricity (Kelly, 1971a, 1971b) and recent evidence suggests that information processing may even be faster in the periphery (Carrasco, McElree, Denisova, & Giordano, 2003). We sought to test whether these differences in the sensitivity to spatial and temporal modulation as a function of eccentricity might also affect spatial interference among moving elements. We therefore measured how an observer's ability to detect the direction of motion of a textured element was affected by the presence of nearby moving elements.

It is now widely agreed that the perception of motion over large areas of visual space is based on a hierarchical process of integration over successively increasing size. Unidirectional motion signals at a limited spatial scale are first encoded by motion detectors with small receptive fields, such as those observed in area V1 of the primate cortex (Hubel & Wiesel, 1968). Behavioural studies of motion summation in human observers confirm that the motion of single drifting Gabor patches is integrated by detectors with small receptive fields that scale with the target wavelength ($c$ 2′ to 7 deg, Anderson & Burr, 1987). Numerous behavioural (Bex & Makous, 1997; Bex, Metha, & Makous, 1998; Bex, Metha, & Makous, 1999; Burr, Morrone, & Vaina, 1998; Dakin & Bex, in press; Freeman & Harris, 1992; Gurney & Wright, 1996; Lappe, Bremmer, & van den Berg, 1999; Lappe & Rauschecker, 1995; Meese, 2000; Meese & Harris, 2001; Morrone, Burr, & Di Pietro, 1999; Morrone, Burr, & Vaina, 1995; Regan & Beverly, 1978; Snowden & Milne, 1996, 1997; Verghese & Stone, 1995, 1996; Wilkinson et al., 2000; Wilson & Wilkinson, 1998; Wilson, Wilkinson, & Asaad, 1997) and electrophysiological (Duffy & Wurtz, 1991, 1993; Graziano, Andersen, & Snowden, 1994; Kim, Mulligan, & Sherk, 1997; Orban, Lagae, Raiguel, Xiao, & Maes, 1995; Saito, Tanaka, Isono, Yasuda, & Mikami, 1989; Tanaka & Saito, 1989) studies have shown that later stages of visual processing involve detectors with receptive fields of increasing size that specialise in the detection of complex global patterns that form the primitives of optic flow (Koenderink, 1986). This suggests that the visual system differentially integrates different motion configurations and led us to speculate that the global pattern of motion may also affect the magnitude or the spatial extent over which spatial interference might be observed. To test this conjecture, we manipulated the directions of motion of groups of crowding elements so that their combined

motions formed different global patterns of translation, rotation, expansion/contraction or random motion.

## 2. Experiment 1: Acuity and spatial interference with drifting Gabor stimuli

### 2.1. Methods

#### 2.1.1. Apparatus

Stimuli were generated on a Macintosh G4 computer with software adapted from the VideoToolbox routines (Pelli, 1997) and were displayed on a LaCie Electron-Blue 22′ monitor at a frame rate of 75 Hz and a mean luminance of 50 cd/m$^2$. The display measured 36 cm (1152 pixels) horizontally, 27.2 cm (870 pixels) vertically and was 230, 115 cm or 57 cm from the observer, in an otherwise dark room. The luminance of the display was linearized with pseudo-12-bit resolution (Pelli & Zhang, 1991) in monochrome and calibrated with a Minolta photometer. Images were presented in greyscale by amplifying and sending the same 12-bit monochrome signal to all RGB guns of the display.

#### 2.1.2. Stimuli

The target stimulus was a horizontal or vertical Gabor patch that was the product of a circular Gaussian envelope and an oriented sinusoid:

$$G(x,y) = \exp\left(-\frac{(x^2+y^2)}{2\sigma^2}\right) \times \cos\left[2\pi\frac{(\cos\theta x + \sin\theta y)}{\rho} + \phi\right] \quad (1)$$

where $\theta$ determines the orientation, $\rho$ the spatial frequency and $\phi$ the phase of the sinusoid. Unless otherwise stated, the Michelson contrast of the targets was 50%. The standard deviation of the Gaussian window ($\sigma$) was fixed at half the wavelength of the carrier. The starting phase ($\phi$) of the sinusoidal carrier was random on any trial and was changed by 9.6 deg on successive video frames to produce animation at 2 Hz. The orientation of the carrier grating was varied to produce up, down, left or right motion within the stationary Gaussian window. Illustrations of single animation frames of the stimuli are shown in Fig. 1 and are drawn to scale so that 1.5–2 cycles of the carrier grating were visible within the Gaussian window. The target was presented in the centre of the display (at the locus of luminance calibration) and a black (<1 cd/m$^2$) fixation cross was presented 256 pixels to its right. The observer's viewing distance was varied from 230, 115 to 57 cm so that the eccentricity of the target was 2, 4 or 8 deg, respectively in the nasal visual field (to avoid the blind spot).

The observers were the authors (PB and SD) who are both experienced psychophysical observers with visual acuity of 6/6 or better and both practised the task extensively before formal data collection. Observers viewed the display monocularly with an eye-patch covering their non-dominant eye. Their task in all experiments was to fixate the cross and to identify the direction of motion of the target (up down, left or right) by pressing one of four buttons on a response box. Auditory feedback was provided following incorrect responses.

Stimuli were presented for 160 ms within a raised cosine temporal envelope lasting 26 ms. This brief duration prevented observers from making an involuntary eye movement to the target as these take 150–200 ms to initialise and execute to a known location (Carpenter, 1988).

#### 2.1.3. Procedure

*2.1.3.1. Acuity.* Direction acuity thresholds were first measured by varying the spatial frequency of the target Gabor in a four alternative direction identification task. The target spatial frequency was under the control of a QUEST staircase (Watson & Pelli, 1983) that concentrated stimuli at a spatial frequency producing 75% correct responses. Note that as the standard deviation of the Gaussian envelope was in fixed proportion to carrier wavelength, target size decreased as spatial frequency increased. Direction acuity thresholds were measured at eccentricities of 2, 4 and 8 deg, in random order, by changing the viewing distance between runs. The raw data from at least four runs of 32 trials were combined and fitted with a cumulative normal function by least $\chi^2$ fit, from which direction acuity thresholds were determined at the 75% correct level together with 95% confidence intervals on this point by standard methods (Press, Teukolsky, Vetterling, & Flannery, 1992).

*2.1.3.2. Spatial interference.* Spatial interference was measured in a four alternative direction identification task in which observers identified the direction of motion (up, down, left, right) of a target Gabor that was surrounded by four flanking Gabors that were either drifting or counter-phase flickering. We originally planned to set the spatial frequency of the target Gabor close to a value that just supported its unflanked direction identification in analogy to the standard procedure of crowding studies with static stimuli. However, we found that the direction identification task was impossible with flanking elements present at almost any separation, so we instead set the target spatial frequency at twice the direction acuity threshold. It was therefore very easy to detect the direction of this target in isolation, but with four flanking elements present the task was difficult.

The spatial frequency of the target and flanking Gabors was the same and was fixed at twice the direction acuity threshold estimated in the acuity tasks at each eccentricity. We have shown elsewhere that contrast detection thresholds are the same for expanding,

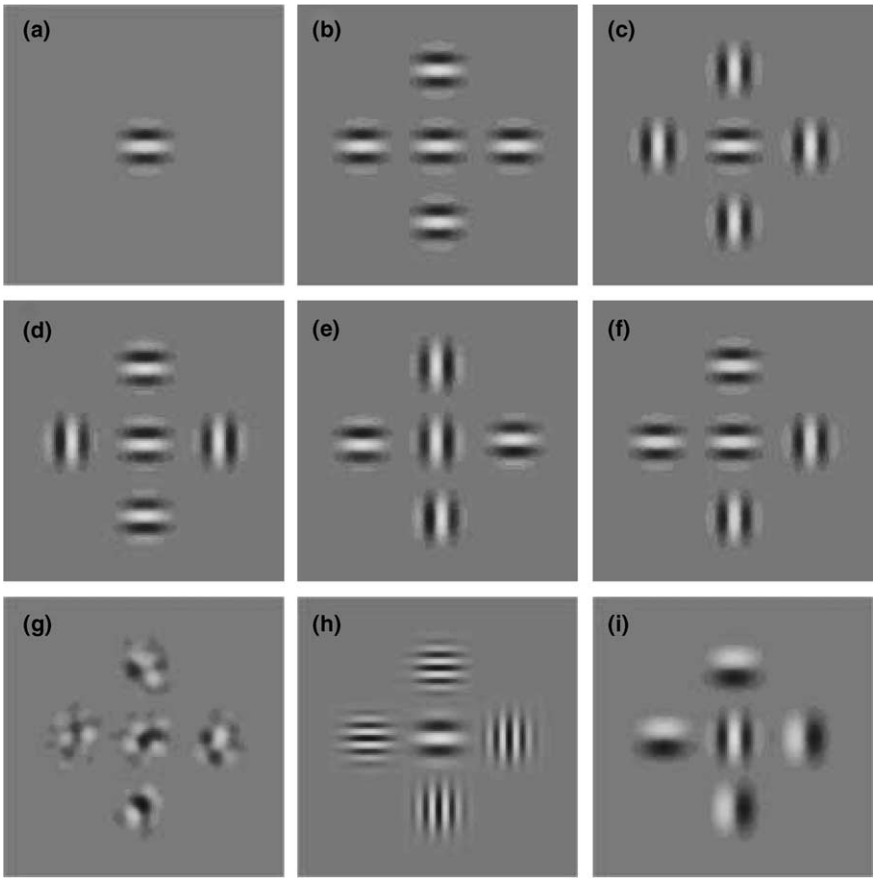


Fig. 1. Illustrations of the stimuli. Observers were required to identify the direction of motion (up, down, left right) of a Gabor element (a horizontal or vertical grating drifting within a stationary Gaussian envelope). (a) Single targets were presented in acuity conditions. Direction acuity threshold was the highest spatial frequency, that supported the 75% correct identification of the direction of an isolated Gabor element. (b)–(i) Four drifting flanking elements were positioned around the target on crowding tasks. The resultant Spatial Interference Zone was the centre–centre spacing between each flanking element and the central target element that restored direction identification of the target element to 75% correct. The directions/orientations of the four flanking elements were arranged to form global patterns of (b) parallel translation; (c) orthogonal translation; (d) rotation; (e) radial or (f) random motion. (g) Isotropic band-pass filtered noise targets were used in Experiment 2 to remove orientation cues. Spatial frequency tuning was measured with (h) high and (i) low spatial frequency flanking elements. See text for details.

contracting, rotating and translating patterns composed of similar elements to those employed in the present manuscript (Bex et al., 1998) and so no additional contrast scaling was required to equate the visibility of the flanking elements. The temporal frequency of target and flanking elements was fixed at 2 Hz. The extent of spatial interference was measured by measuring sensitivity to the direction of motion of the target element as a function of the centre–centre separation between target and flanking Gabors. The directions of motion of the four flanking elements were set to form the following global patterns:

A. *Translation*: all four flankers moved in the same direction (up, down, left or right). This direction was determined randomly from trial to trial. In separate conditions the relative directions of the target and flanking elements were either the same (condition 1, Fig. 1b), orthogonal (condition 2, Fig. 1c) or opposite (condition 3, Fig. 1b).
B. *Complex motion*: each flanker moved in a different direction. In separate conditions flankers formed a global pattern of rotation (condition 4, either clockwise or counter-clockwise, at random across trials, Fig. 1e) expansion (condition 5, Fig. 1d) contraction (condition 6, Fig. 1d) or random motion (condition 7, any random combination of up, down, left and right flankers that was not rotational or radial, Fig. 1f). The absolute direction of the target was randomised across trials.
C. *Flicker*: the contrast of each flanker was sinusoidally reversed at 2 Hz to produce counter phase flicker. In separate conditions the orientations of the flanks were: all the same orientation with a parallel target (condition 8, Fig. 1b), all the same orientation with an orthogonal target (condition 9, Fig. 1c), in a radial configuration with randomised target direction (condition 10, Fig. 1d), or in a circular configuration with randomised target direction (condition 11, Fig. 1e).

Illustrations of single animation frames of the stimuli are shown in Fig. 1. Note that single animation frames are the same for more than one condition and conditions differ only with the directions of element motion, direction arrows have been drawn on the illustrative captions below the results to help differentiate conditions.

To minimise adaptation effects and to prevent the observer from anticipating the direction of target motion, the eleven conditions were randomly interleaved in a single run. The separation between target and flanking elements was under the control of a QUEST staircase (Watson & Pelli, 1983) that concentrated observations at a separation producing 75% correct responses for detecting the direction of motion of the central target Gabor. The raw data from at least four runs of 32 trials were combined and we confirmed by inspection that performance ranged from chance to 100% correct in all cases. As in the acuity condition, combined data were fit with a cumulative normal function from which the extent of spatial interference was determined at the spacing that produced 75% correct identification of the target direction. 95% confidence intervals on this point were estimated by standard methods (Press et al., 1992) and are indicated by error bars.

## 2.2. Results

### 2.2.1. Acuity

Fig. 2 shows direction acuity in c/deg for two observers (see legend) at three eccentricities, indicated on the *x* axis. Direction acuity is defined as the highest spatial frequency grating drifting at 2 Hz whose direction (up, down, left, or right) observers were able to identify on 75% trials. Error bars show ±95% confidence intervals. Results indicate a conventional decline in spatial frequency acuity with eccentricity. These thresholds were used to scale the spatial frequency of target and flank stimuli in the crowding experiments to ensure equal visibility of elements under all conditions.

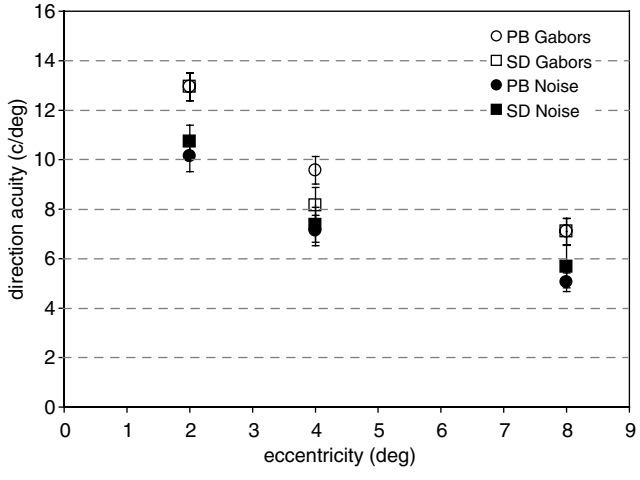


Fig. 2. Direction acuity for two observers. Direction acuity threshold was defined as the highest spatial frequency that supported element direction discrimination on 75% trials. Stimuli were isolated Gabors (open symbols) or Gaussian-windowed patches of band-pass filtered noise (filled symbols). Error bars show 95% confidence intervals.

### 2.2.2. Spatial interference

Figs. 3–5 show the extent of spatial interference, in degrees of visual angle, for two observers at three eccentricities (2, 4 and 8 deg; see legend). Error bars show 95% confidence intervals. In this section, we treat the eleven conditions of flanker motion separately, but the data were collected in a single run. Across all conditions, spatial interference increased with eccentricity, in line with many previous studies (Bex et al., 2003; Bouma, 1970; Chung et al., 2001; Hess et al., 2000b; Jacobs,

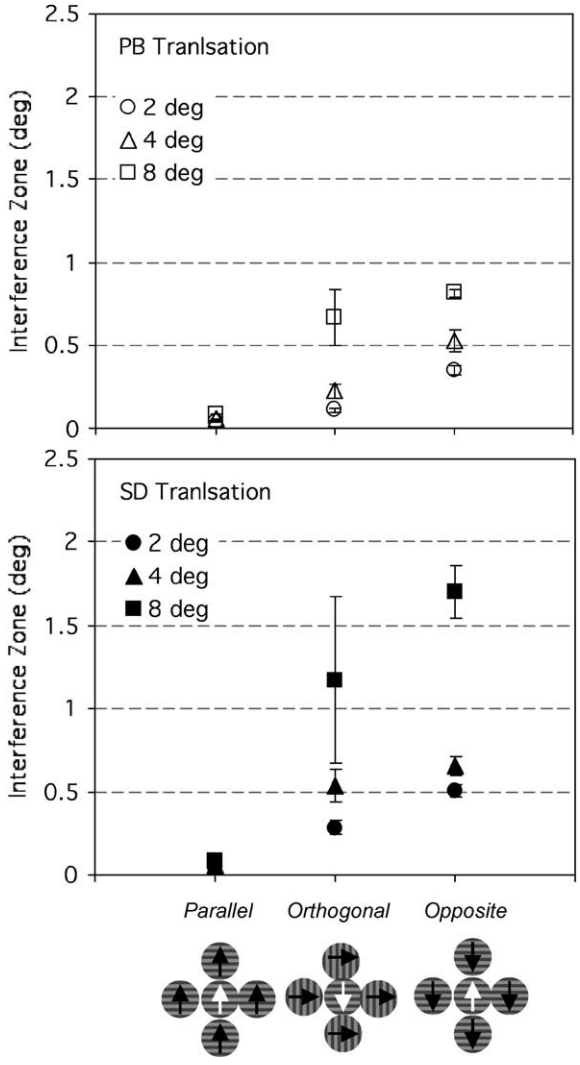


Fig. 3. The spatial extent of crowding induced by translating flanks. Interference zones are defined as the centre–centre spacing between the target and each flanking element that produced 75% correct direction identification. Error bars show 95% confidence intervals.

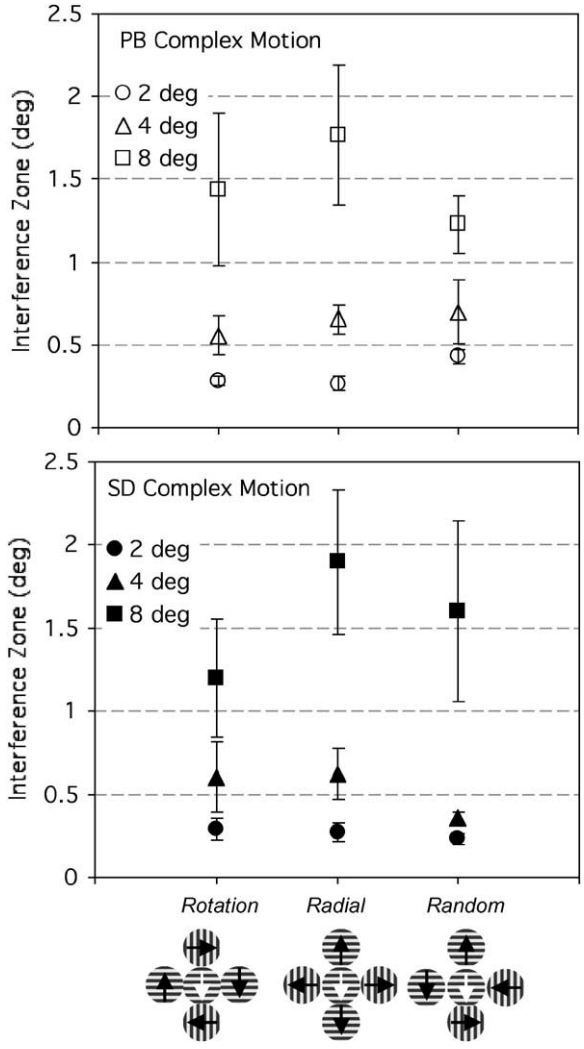


Fig. 4. The spatial extent of crowding induced by flanks undergoing complex motion. As Fig. 3, except flanking elements could either form a global pattern of rotation, expansion, contraction or random motion.

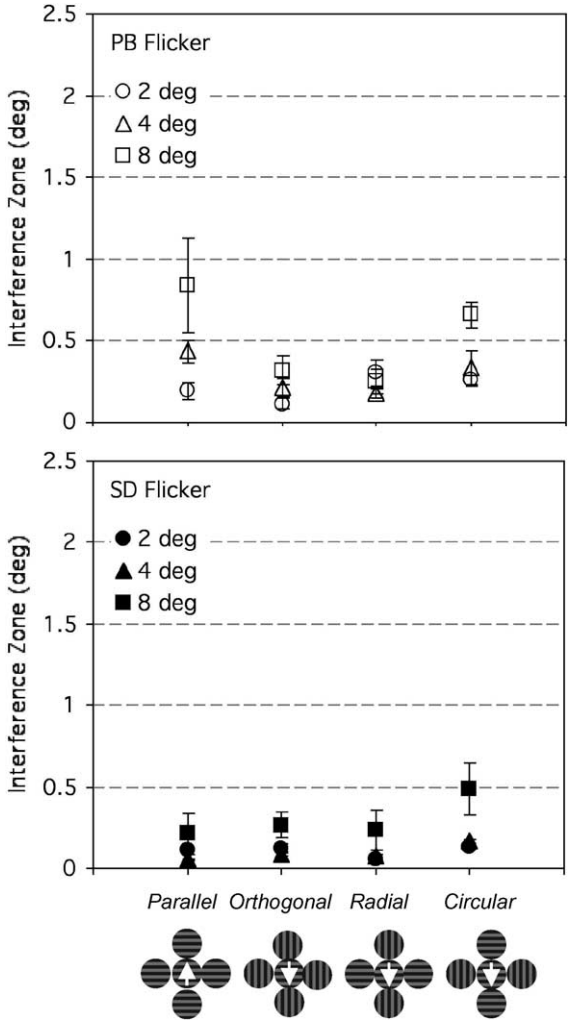


Fig. 5. The spatial extent of crowding induced by counter-phase flickering flanks. As Fig. 3, except flanking elements were counter-phase flickering and were arranged in a parallel, orthogonal, circular or radial configuration around the target.

1979; Latham & Whitaker, 1996; Loomis, 1978; Strasburger, Harvey, & Rentschler, 1991; Toet & Levi, 1992; Wolford & Chambers, 1984).

As we used Gabor stimuli, the tails of the elements were allowed to overlap. Based on a conservative estimate of 2 visible cycles (see Fig. 1) and ignoring contrast attenuation in the tails of the Gaussian window, the radii of the elements were 9.2′ at 2 deg eccentricity, 13.3′ at 4 deg eccentricity and 17.14′ at 8 deg eccentricity. For all except parallel translating conditions (in which we report no crowding in Experiment 1) the element radii are much smaller than the extent of spatial interference and indicate that crowding occurred even when there was a clear gap between the target and flankers.

Fig. 3 shows that there was effectively no spatial interference for conditions in which all flanks moved in the same direction to form a global pattern of translation. We return to this point below. Spatial interference was present when the target and flanking elements moved in orthogonal directions and was even greater when the target and flanking elements moved in opposite directions.

Fig. 4 shows the extent of spatial interference for conditions in which the flanks all moved in a different direction, forming global patterns of rotational, radial or random complex motion. As there were no systematic differences between results derived with the two directions of optic flow patterns (clockwise and anti-clockwise rotation, expanding and contracting radial motion) these data were combined across directions. At all eccentricities, spatial interference was greater with complex motion flanking stimuli than with translational flanks, but no systematic differences among the complex patterns was evident.

Fig. 5 shows the extent of spatial interference for conditions in which the flanks counter-phase flickered. Their orientations were manipulated to form global

arrangements of parallel, radial, circular or random structure. Counter-phase flickering flanks produce less spatial interference than drifting flanks (except for same direction conditions) and there was no systematic effect of their orientation configuration. This observation could be attributed, at least in part, to the lower contrast of each of the drifting components forming the counter-phase flickering patch.

## 3. Experiment 2: Acuity and spatial interference with noise stimuli

Limitations arise from the use of the Gabor stimuli used in Experiment 1 that restrict the conclusions that can be drawn from the results. We randomly interleaved all conditions in a single run to minimise the observer's ability to use the structure or direction of the flanking elements to influence their responses. However, it is possible that observers reported the direction of one of the flanking elements when they could not detect the direction of the target (Chastain, 1982; Ortiz, 2001). Although this problem is avoided with the complex motion stimuli in which the flanks contain all four directions, it could explain why we found little or no spatial interference when target and flanking elements moved in the same direction (Fig. 3, left data), because reporting the direction of any element, target or flank, produces a correct response. To avoid this problem, we adopted a true 4AFC task in which the observer identified the interval containing specified target direction (e.g., 'left') among four intervals that contained each possible target direction (up/down/left/right).

It is also possible that the static orientation cues presented by Gabor micro-patterns in the orthogonal condition could have affected the results. Our fitting procedure assumed a guess rate of 25% (up/down/left/right), but if observers could detect the orthogonal target orientation (for example by pop-out; Beck, 1982; Julesz, 1984; Treisman, 1987, chapter 35), but not its direction, the guess rate would increase to 50% (up or down if horizontal; left or right if vertical). It is possible that this contributed to the difference between orthogonal and same orientation conditions. In practice this is unlikely because this potential cue is present in flickering surround gratings yet we observed no systematic difference for flickering gratings of any orientation combination. Furthermore, the guess rate on psychometric functions was around 25% instead of 50%. However, in order to avoid these potential confounds between the direction and orientation of target and flanks, we repeated Experiment 1 with isotropic band-pass filtered noise drifting within the static Gaussian envelopes.

Uniform noise was digitally filtered (Press et al., 1992) with logarithmic exponential filters. These filters have the advantage of sharper spatial frequency tuning than other candidates such as Laplacian of Gaussian filters and are defined in the Fourier domain by

$$A(f) = \exp\left(\frac{|\ln(f/F_{\text{peak}})|^3 \ln 2}{(b_{0.5} \ln 2)^3}\right) \quad (2)$$

where $F_{\text{peak}}$ specifies the peak frequency and $b_{0.5}$ the half bandwidth of the filter in octaves, which was fixed a 0.5 octaves (full bandwidth was one octave).

Direction acuity was measured as in Experiment 1 by varying the peak spatial frequency of the target in a single interval 4 alternative direction identification task, under the control of a QUEST staircase (Watson & Pelli, 1983). Thresholds at three eccentricities (2, 4 or 8 deg) were measured in random order by changing the viewing distance between runs. The drift speed of the noise carrier was fixed at 1 pixel/frame, with the consequence that the peak temporal frequency varied with the peak spatial frequency of the noise and speed increased with eccentricity (0.6, 1.2 or 2.3 deg/s at 2, 4 or 8 deg eccentricity, respectively) as the viewing distance was changed. However, the target and flanking elements were always the same spatial and temporal frequency as each other so comparisons at a given eccentricity are at a fixed speed. Furthermore, we show in Experiment 3 that spatial interference is broadly tuned for temporal frequency, so that it is not likely that this difference affected our results. However, this limitation does prevent direct comparison of crowding *magnitude* across eccentricity.

We adopted a 4AFC procedure to measure spatial interference. In this task, there were four temporal intervals, one for each of the target directions (up/down/left/right), in random order and separated by 250 ms. The motion of the four flanking elements was similar across the four intervals, following the same directional conditions of translation and complex motion as in Experiment 1, with the exception that counter-phase flicker was not included. The observer's task was to identify which of the four intervals contained a target drifting in a specified direction. The specified target direction was randomly selected and then fixed within each run. Adaptation at the target location should be minimal since all four target directions were presented in random order each trial. Adaptation effects on both target and flanks were avoided by randomly interleaving all flank conditions within a single run. All other parameters were similar to those employed in Experiment 1.

### 3.1. Results

Direction acuity performance with noise carriers are included in Fig. 2 (filled symbols), along with equivalent data for grating carriers (open symbols). These data show the fall-off in acuity with eccentricity and were used to scale the stimuli in the crowding experiments to twice threshold carrier-wavelength (as in Experiment 1).

Figs. 6 and 7 show the extent of spatial interference (in degrees of visual angle) for two observers at eccentricities of 2, 4 and 8 deg. We treat the six conditions of flanker motion separately, but recall that the data were collected in a single run. Across all conditions, spatial interference increased with eccentricity. In this Experiment, 4AFC and noise carriers prevented observers from achieving a correct response by reporting the direction of any flanking element and isotropic noise carriers eliminated orientation interactions between target and flanking stimuli. Under these conditions, spatial interference for translating flanks were present for all surrounds configurations and there were no systematic differences between same, orthogonal or opposite target and flank directions. However, note that even with our 4AFC task it is still possible that observers identified the interval containing same direction flanks not by detecting the motion of the target element. For example if observers could reliably determine the interval containing orthogonal and opposite direction flanks, the same direction condition is necessarily the remaining interval. It is therefore possible that we may still have underestimated the extent of spatial interference for translating flanks moving in the same direction as the target. With noise carriers, spatial interference was still greater for complex moving flank configurations than for translating flank configurations (with the possible exception of same-direction translation). Random direction flanks were still as effective as rotating or expanding/contracting flanks.

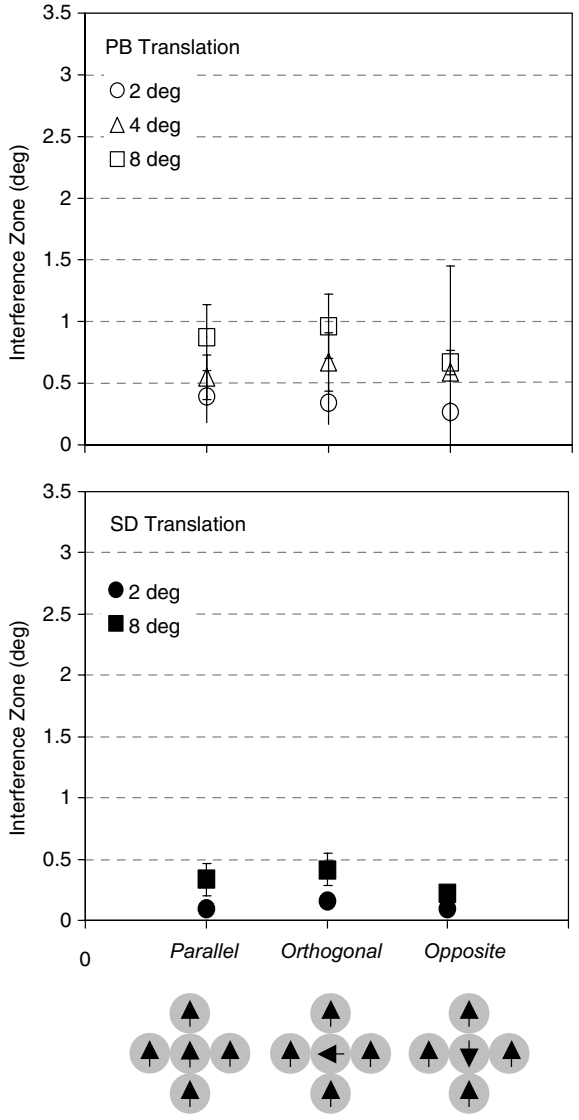


Fig. 6. Crowding among drifting noise elements forming a global pattern of translation. The direction of motion is indicated on the *x* axis. Details as Fig. 3.

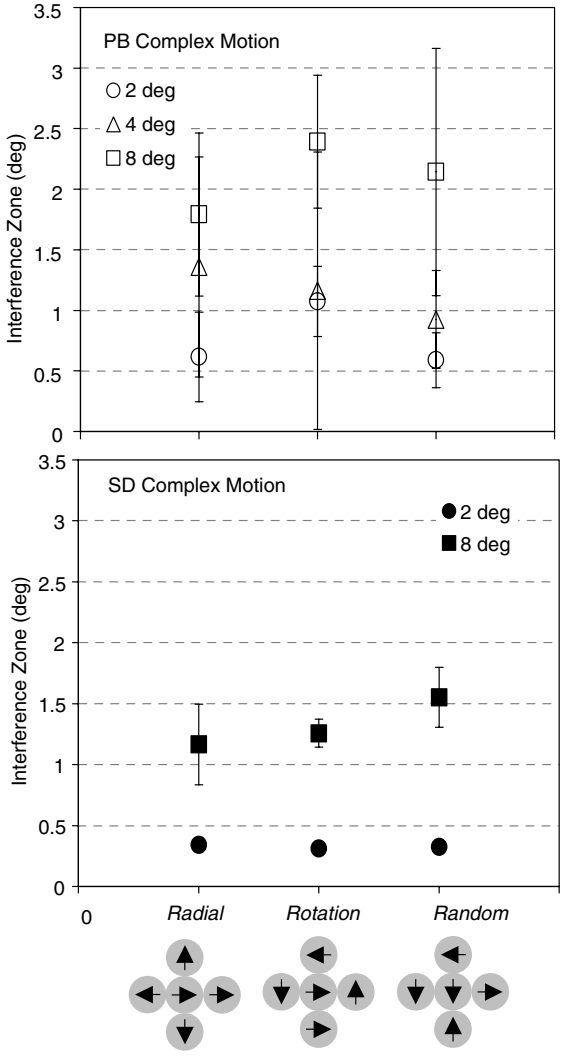


Fig. 7. Crowding among drifting noise elements forming a global pattern of complex motion. The direction of motion is indicated on the *x* axis. Details as Fig. 3.

## 4. Experiment 3: Spatial and temporal frequency tuning of spatial interference

In order to examine the underlying connectivity of the interactions among nearby motion detectors, we estimated the spatial and temporal frequency tuning of motion spatial interference. The extent of spatial interference was measured, at 4 deg eccentricity, for a target of fixed spatial and temporal frequency as a function of the spatial or temporal frequency of the flanking stimuli. We used a single interval direction identification task with random direction flanking Gabor elements, (condition 4 in Section 2.1). The flanking elements in this stimulus contain all target directions and orientations and therefore avoid some potential confounds between the target and flank orientations and directions discussed above, except the possibility of that knowledge of the target orientation would restrict the directions to 2 instead of 4. This single interval task was faster than the 4AFC task which assisted in maintaining observer concentration over the run. The spatial (5 c/deg) and temporal (2 Hz) frequency of the target element was the same as in Experiment 1 for this eccentricity.

### 4.1. Results

Fig. 8 shows extent of spatial interference as a function of the spatial frequency of Gabors drifting at 2 Hz flanking a 5 c/deg centre target drifting at 2 Hz. Open symbols plot data from conditions in which the Michelson contrast of the target and flanks was 50%. Filled symbols plot data from conditions in which the Michelson contrasts of target and flank elements were equated for visibility ($2\times$ threshold detection contrast). Contrast direction identification threshold was measured as for the direction acuity task in Experiment 1, except that the spatial frequency of the target was fixed and its contrast was adjusted to determine the contrast required for observers to identify the target direction correctly on 75% trials. In both cases, spatial interference was greatest for flanking elements that were lower in spatial frequency than the target, i.e., motion crowding was low-pass tuned for spatial frequency.

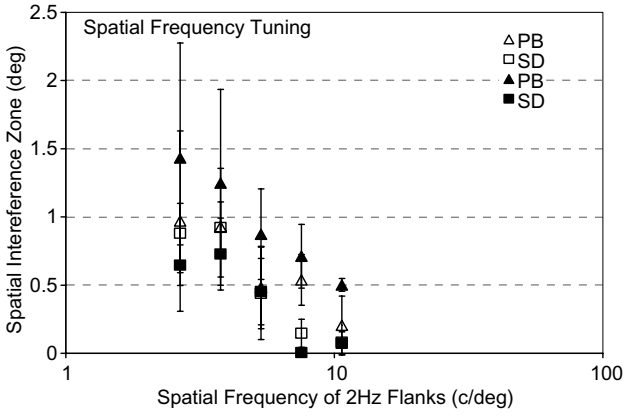


Fig. 8. Spatial frequency tuning of motion crowding. Details as Fig. 3, except that a 5 c/deg central target was surrounded by four flanking elements forming a random global pattern of motion (all four directions in random order) of the spatial frequency shown on the $x$ axis.

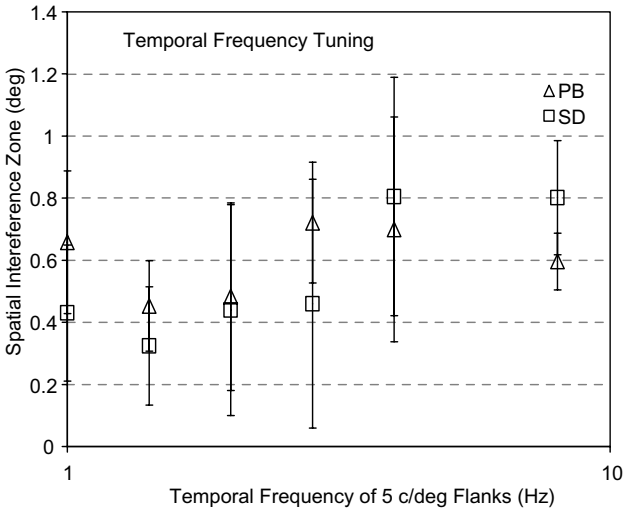


Fig. 9. Temporal frequency tuning of motion crowding. Details as Fig. 3, except that a 5 c/deg central target was surrounded by four flanking elements forming a random global pattern of motion (all four directions in random order) of the temporal frequency shown on the $x$ axis.

Fig. 9 plots spatial interference as a function of the temporal frequency of 5 c/deg drifting Gabors flanking a centre target of 5 c/deg, drifting at 2 Hz. There was little difference in contrast direction identification threshold as a function of target temporal frequency so we did not need to equate the visibility of target and flank elements. Spatial interference was approximately the same for all flanking temporal frequencies, i.e., motion crowding is broadly tuned for temporal frequency.

## 5. General discussion

### 5.1. Acuity, crowding and motion

We first measured the resolution limit for drifting targets so that crowding targets could be placed near their resolution threshold. In line with many previous studies, we found that resolution decreased with eccentricity (Aubert & Forster, 1857). It is standard practice in studies of crowding to place the resolution target near threshold (Bouma, 1970; Flom et al., 1963; Townsend et al., 1971). We had originally planned to present the target at a size producing 90% correct direction discrimination, but found that observers were unable to identify the direction of motion when such a target was

surrounded by four drifting flanking Gabors, even when there was a considerable separation between them. We therefore elected to present the target at a wavelength that was twice resolution threshold. Several studies have shown that while the extent of spatial interference scales with spatial frequency in foveal vision (Chung et al., 2001; Levi, Hariharan, et al., 2002) it is approximately invariant of target size or spatial frequency (Chung et al., 2001; Levi, Hariharan, et al., 2002; Tripathy & Cavanagh, 2002) in peripheral visual field. As our data were collected in the peripheral visual field, the results are therefore not likely to have been affected by the particular target spatial frequency we selected.

In line with many previous studies we also found that crowding effects increased with eccentricity (Bouma, 1970; Chung et al., 2001; Hess et al., 2000b; Jacobs, 1979; Latham & Whitaker, 1996; Loomis, 1978; Strasburger et al., 1991; Toet & Levi, 1992; Wolford & Chambers, 1984). Unlike previous studies (including studies that used drifting targets (Aubert & Forster, 1857; Bex et al., 2003), the present task did not require observers to make a spatial discrimination (i.e., letter identity or orientation). It is well known that while spatial resolution for static images decreases with eccentricity (Aubert, 1857), sensitivity to motion or flicker is relatively invariant of eccentricity (McKee & Nakayama, 1984; Waugh & Hess, 1994; Wright & Johnston, 1983)—and in the case of critical flicker fusion threshold, sensitivity can be higher in the peripheral than foveal visual field (Kelly, 1971a, 1971b). It was therefore unclear if crowding of a direction discrimination task (that did not require identification of spatial form) would increase with eccentricity. We report that it does.

### 5.2. Tuning of crowding

Previous studies of static band-pass filtered letters (Chung et al., 2001) or letters composed of multiple Gabor elements (Levi, Hariharan, et al., 2002) have shown that crowding (like masking) is band-pass tuned for spatial frequency in fovea and broadly tuned for spatial frequency in peripheral visual field. Our data suggest that directional crowding is low-pass tuned for spatial frequency. In other motion-based tasks, low-pass spatial frequency tuning and broad temporal frequency tuning has been observed (Bex & Dakin, 2002).

The data presented above are consistent with these results. We found low pass tuning of similar magnitude when either the physical or the effective (fixed multiple of detection threshold) contrast of the target and flanking elements were equated. As contrast threshold increased with spatial frequency, the relative physical contrast of the flanks increased with their spatial frequency. When there is a contrast difference between static target and flank elements of the same spatial structure, there can be a release from crowding that has been attributed to segmentation (Kooi et al., 1994), although others have reported that crowding effects increase monotonically with the contrast of the flanks (Kothe & Regan, 1990). Our target and flanks differ in spatial frequency content; under these conditions we also found no evidence of a release from crowding with a difference in either the physical or effective contrast of the flanks.

### 5.3. Motion contrast and motion capture

Electrophysiological and psychophysical studies of motion contrast have shown that surround patterns that move in the same direction tends to reduce neural responses (Allman, Miezin, & McGuinness, 1985; Chiao & Masland, 2003; Frost & Nakayama, 1983; Kastner, Nothdurft, & Pigarev, 1999; Raiguel, Vanhulle, Xiao, Marcar, & Orban, 1995) or reduce behavioural measures of sensitivity (Nakayama & Tyler, 1981; Sachtler & Zaidi, 1995; Shioiri, Ito, Sakurai, & Yaguchi, 2002; van Doorn & Koenderink, 1982; Watson & Eckert, 1994) or adaptation (Bell, Lehmkuhle, & Westendorf, 1976; Day & Strelow, 1971; Strelow & Day, 1971) to motion. Collectively, these results have been modeled by directionally antagonistic centre–surround motion contrast detectors (Murakami & Shimojo, 1993; Nakayama & Loomis, 1974; Nawrot & Sekuler, 1990; Regan & Beverley, 1984; Royden, 1997; Royden, 2002; Sachtler & Zaidi, 1993; Watson & Eckert, 1994) in which responses from adjacent motion detectors tuned to the same direction of motion inhibit one another and/or motion detectors selective for opposite directions facilitate one another. The present results show that the visibility of the direction of motion of a supra-threshold target is impaired most by dissimilar surround directions and this effect is in the opposite direction to that predicted by motion contrast. It is possible that motion of the flanking elements masked the direction of the target by motion capture (Murakami & Shimojo, 1993). The extent of spatial interference increases with eccentricity, like motion capture (Murakami & Shimojo, 1993), however, random motion flanking conditions produced large crowding effects that would not be expected from capture. These factors suggest that the phenomenon observed in the present study is distinct from conventional motion contrast and is therefore best considered spatial interference or crowding.

### 5.4. Implications for low-level models of crowding

Many models of crowding have been proposed. At the earliest stages of perception, it has been suggested that crowding arises from blurring of adjacent features in the retinal image by the eye's optical point spread function (Liu & Arditi, 2000). It is already known that this cannot account for all crowding effects (e.g., because

images presented to different eyes crowd one another; Flom et al., 1963; Tripathy & Levi, 1999), and it cannot explain the present data because similar flanking conditions produce different crowding effects. Another low level model is based on spatial frequency masking by common structure in target and flanking images (Hess et al., 2000a). Once again, it has already been shown that this model cannot account for masking effects in peripheral visual field (for example the observation that target and flanking stimuli of opposite contrast polarity are potent crowders (Hess et al., 2000b) and we note here that this model cannot explain the present data either.

At the next level of visual processing, several authors have noted that crowding effects are greatest among elements of similar spatial (Kooi et al., 1994; Nazir, 1992), spatial frequency (Andreissen & Bouma, 1976; Chung et al., 2001; Hess et al., 2000a; Kooi et al., 1994) or orientation (Levi, Klein, et al., 2002) structure. These results are consistent with masking effects within selective visual channels. If we attempt generalise this approach to account for direction crowding, one would expect greater crowding effects between target and flanking elements that move in the same direction. However, we observe crowding effects of approximately the same magnitude for all translating flank conditions, including same-, orthogonal-, and opposite-direction configurations (Fig. 6), with the caveat that a 4AFC paradigm does not exclude the possibility that same direction is detected by default. Furthermore, we also report that flanks of lower spatial frequency than the targets are the most effective (Fig. 7). Neither of these findings is consistent with masking.

### 5.5. Implications for higher-level models of crowding

#### 5.5.1. Positional confusions of target and flank elements

An analysis of the apparent identity of letters presented under crowded conditions shows that observers' responses are not random. Observers are more likely to report the identity of one of the flanking letters than other letters of equal probability (Chastain, 1982; Ortiz, 2001). This suggests that instead of the target identity being lost, masked or averaged, its position (and therefore its identity) is confused with that of one of the flanking elements. However, our data are not consistent with this explanation. If this effect were to account for direction crowding, we would expect no crowding for same direction translating flanks in our 4AFC tasks. This is because the observer could discriminate the interval containing five elements of the same direction from the other three intervals that contain four same and one different direction.

#### 5.5.2. Compulsory form integration

It has recently been shown that an observer's ability to discriminate the orientation of a tilted Gabor can be impaired by nearby Gabors of differing orientation, an effect similar to crowding of letter identity (He et al., 1996; Parkes et al., 2001; Wilkinson et al., 1997). While the orientation of the crowded target grating is not detectable, it can generate local, orientation-specific after-effects (He et al., 1996) and it contributes to the orientation, contrast or spatial frequency of the group by a quantity equivalent to simple averaging (Parkes et al., 2001; Wilkinson et al., 1997). Based on these data, Wilkinson et al. (1997) and Parkes et al. (2001) propose that this and possibly other forms of crowding are caused by "compulsory averaging" of stimulus information within the smallest receptive fields available at a given eccentricity. Although these models were developed to account for orientation discrimination, if it represents a general model of crowding then we should be able to apply it to our motion task. At the most general level, averaging predicts that the higher the directional variability of the flanks the worse the performance, and this is consistent with our observation that radial, rotational and random flanks crowd more than translating flanks. However, note that flanks undergoing complex global motion always contain four orthogonal directions of motion. Four orthogonal directions cancel within an average, so that the mean of the quintet is always that of the target element. According to a simple compulsory averaging model, we should observe little or no crowding for our complex motion conditions, but we actually observe the greatest crowding effects for these stimuli.

We propose that in order to accommodate our findings, the averaging model must to modified to allow for the presence of a random-direction/zero-mean "pedestal". Alternatively, averaging might be restricted to occur within a narrow range of directions (for example, only within channel). In this case, a similar pedestal or orientation effect would also be expected for orientation crowding; this has yet to be examined.

#### 5.5.3. Crowding from meaningful global configurations

It has recently been suggested that while crowding inevitably involves masking effects that have been modelled with linear filters at a first stage of visual processing, it also involves a subsequent stage in which the visual system pools information over a region that increases with eccentricity (Chung et al., 2001). Our results are consistent with this suggestion. Our observation that the spatial extent of crowding is larger for complex motion configurations is consistent with the large receptive fields (up to 60 deg) that have been reported for optic flow detectors (Burr et al., 1998). Under this view, though, it is less clear why random surround flank combinations should crowd as much as radial and rotational surrounds. The random configurations contained direction contrast and motion shearing among the crowding elements could also promote integration across large areas. We therefore speculate that crowding arises from

second stage integration processes in the visual system and that the spatial extent of such pooling increases with eccentricity and also depends on the configurations of the components of the retinal image.

## Acknowledgments

We are grateful to Professor Mark Georgeson for suggesting the 4AFC task employed in Experiment 2. The research was supported by the Wellcome Trust and by the Biotechnical and Biological Sciences Research Council.

## References

Allman, J., Miezin, F., & McGuinness, E. (1985). Stimulus specific responses from beyond the classical receptive field: Neurophysiological mechanisms for local–global comparisons in visual neurons. *Annual Review of Neuroscience, 8*, 407–430.

Anderson, S. J., & Burr, D. C. (1987). Receptive field size of human motion detection units. *Vision Research, 27*(4), 621–635.

Andreissen, J. J., & Bouma, H. (1976). Eccentric vision: Adverse interactions between line segments. *Vision Research, 16*, 71–78.

Aubert, H., & Forster, B. (1857). Beiträge zur kenntniss des indirekte sehens (I) untersuchungen über den raumsinn der retina (Contributions to the knowledge of indirect seeing (I) investigating the spatial localisation of the retina). *Archive für Ophthalmologie, 3*, 1–37.

Beck, J. (1982). Textural segmentation. In J. Beck (Ed.), *Organisation and representation in perception*. Hillsdale, NJ: Erlbaum.

Bell, H., Lehmkuhle, S. W., & Westendorf, D. H. (1976). On the relation between visual surround and motion aftereffect velocity. *Perception and Psychophysics, 20*, 13–16.

Bex, P. J., & Dakin, S. C. (2002). Comparison of the spatial-frequency selectivity of local and global motion detectors. *Journal of the Optical Society of America a—Optics Image Science and Vision, 19*(4), 670–677.

Bex, P. J., Dakin, S. C., & Simmers, A. J. (2003). The shape and size of crowding for moving targets. *Vision Research, 43*(27), 2895–2904.

Bex, P. J., & Makous, W. (1997). Radial motion looks faster. *Vision Research, 37*(23), 3399–3405.

Bex, P. J., Metha, A. B., & Makous, W. (1998). Psychophysical evidence for a functional hierarchy of motion processing mechanisms. *Journal of the Optical Society of America A, 15*(4), 769–776.

Bex, P. J., Metha, A. B., & Makous, W. (1999). Enhanced motion aftereffect for complex motions. *Vision Research, 39*(13), 2229–2238.

Bouma, H. (1970). Interaction effects in parafoveal letter recognition. *Nature, 226*, 177–178.

Burr, D. C., Morrone, M. C., & Vaina, L. M. (1998). Large receptive fields for optic flow detection in humans. *Vision Research, 38*(12), 1731–1743.

Carpenter, R. H. S. (1988). *Movements of the eyes*. Lodon: Pion.

Carrasco, M., McElree, B., Denisova, K., & Giordano, A. M. (2003). Speed of visual processing increases with eccentricity. *Nature Neuroscience, 6*(7), 699–700.

Chastain, G. (1982). Confusability and interference between members of parafoveal letter pairs. *Perception Psychophysics, 32*(6), 576–580.

Chiao, C. C., & Masland, R. H. (2003). Contextual tuning of direction-selective retinal ganglion cells. *Nature Neuroscience, 6*(12), 1251–1252.

Chung, S. T. L., Levi, D. M., & Legge, G. E. (2001). Spatial-frequency and contrast properties of crowding. *Vision Research, 41*(14), 1833–1850.

Dakin, S. C., & Bex, P. J. (in press). Summation of concentric orientation structure: Seeing the glass or the window? *Vision Research*.

Day, R. H., & Strelow, E. R. (1971). Reduction or disappearance of visual aftereffect of movement in the absence of patterned surround. *Nature, 230*, 55–56.

Duffy, C. J., & Wurtz, R. H. (1991). Sensitivity of MST neurons to optic flow stimuli. I. A continuum of response selectivity to large-field stimuli. *Journal of Neurophysiology, 65*(6), 1329–1345.

Duffy, C. J., & Wurtz, R. H. (1993). An illusory transformation of optic flow fields. *Vision Research, 33*(11), 1481–1490.

Flom, M. C., Weymouth, F. W., & Kahneman, D. (1963). Visual resolution and spatial interaction. *Journal of the optical Society of America, 53*, 1026–1032.

Freeman, T. C. A., & Harris, M. G. (1992). Human sensitivity to expanding and rotating motion: Effects of complementary masking and directional structure. *Vision Research, 32*(1), 81–87.

Frost, B. J., & Nakayama, K. (1983). Single visual neurons code opposing motion independent of direction. *Science, 2*, 744–745.

Graziano, M. S., Andersen, R. A., & Snowden, R. J. (1994). Tuning of MST neurons to spiral motions. *Journal of Neuroscience, 14*(1), 54–67.

Gurney, K., & Wright, M. J. (1996). Rotation and radial motion thresholds support a two-stage model of differential-motion analysis. *Perception, 25*(1), 5–26.

He, S., Cavanagh, P., & Intriligator, J. (1996). Attentional resolution and the locus of visual awareness. *Nature, 383*(6598), 334–337.

Hess, R. F., Dakin, S. C., & Kapoor, N. (2000a). The foveal 'crowding' effect: Physics or physiology? *Vision Research, 40*(4), 365–370.

Hess, R. F., Dakin, S. C., Kapoor, N., & Tewfik, M. (2000b). Contour interaction in fovea and periphery. *Journal of the Optical Society of America a—Optics Image Science and Vision, 17*(9), 1516–1524.

Hubel, D. H., & Wiesel, T. N. (1968). Receptive fields and functional architecture of monkey striate cortex. *Journal of Physiology, 195*, 215–243.

Intriligator, J., & Cavanagh, P. (2001). The spatial resolution of visual attention. *Cognitive Psychology, 43*(3), 171–216.

Jacobs, R. J. (1979). Visual resolution and contour interaction in the fovea and periphery. *Vision Research, 19*, 1187–1195.

Julesz, B. (1984). A brief outline of the texton theory of human vision. *Trends in Neuroscience, 7*, 41–45.

Kastner, S., Nothdurft, H. C., & Pigarev, I. N. (1999). Neuronal responses to orientation and motion contrast in cat striate cortex. *Visual Neuroscience, 16*(3), 587–600.

Kelly, D. H. (1971a). Theory of flicker and transient responses. I. Uniform fields. *Journal of Optical Society of America, 61*(4), 537–546.

Kelly, D. H. (1971b). Theory of flicker and transient responses. II. Counterphase gratings. *Journal of Optical Society of America, 61*(5), 632–640.

Kim, J., Mulligan, K., & Sherk, H. (1997). Simulated optic flow and extrastriate cortex I: Optic flow versus texture. *Journal of Neurophysiology, 77*, 554–561.

Koenderink, J. J. (1986). Optic flow. *Vision Research, 26*(1), 161–179.

Kooi, F. L., Toet, A., Tripathy, S. P., & Levi, D. M. (1994). The effect of similarity and duration on spatial interaction in peripheral-vision. *Spatial Vision, 8*(2), 255–279.

Kothe, A. C., & Regan, D. (1990). Crowding depends on contrast. *Optometry and Vision Science, 67*(4), 283–286.

Lappe, M., Bremmer, F., & van den Berg, A. V. (1999). Perception of self-motion from visual flow. *Trends in Cognitive Sciences, 3*(9), 329–336.

Lappe, M., & Rauschecker, J. P. (1995). An illusory transformation in a model of optic flow processing. *Vision Research, 35*(11), 1619–1631.

Latham, K., & Whitaker, D. (1996). Relative roles of resolution and spatial interference in foveal and peripheral vision. *Ophthalmic and Physiological Optics, 16*(1), 49–57.

Levi, D. M., Hariharan, S., & Klein, S. A. (2002). Suppressive and facilitatory spatial interactions in peripheral vision: Peripheral crowding is neither size invariant nor simple contrast masking. *Journal of Vision, 2*(2), 167–177.

Levi, D. M., Klein, S. A., & Hariharan, S. (2002). Suppressive and facilitatory spatial interactions in foveal vision: Foveal crowding is simple contrast masking. *Journal of Vision, 2*(2), 140–166.

Liu, L., & Arditi, A. (2000). Apparent string shortening concomitant with letter crowding. *Vision Research, 40*(9), 1059–1067.

Loomis, J. M. (1978). Lateral masking in foveal and eccentric vision. *Vision Research, 18*, 335–338.

McKee, S. P., & Nakayama, K. (1984). The detection of motion in the peripheral visual field. *Vision Research, 24*(1), 25–32.

Meese, T. S. (2000). Complex motion detection in human vision. *Spatial Vision, 14*(1), 91–92.

Meese, T. S., & Harris, M. G. (2001). Broad direction tuning for complex motion mechanisms. *Vision Research, 41*(15), 1901–1914.

Millidot, M. (1966). Foveal and extra-foveal acuity with and without stabilized retinal images. *British Journal of Physiological Optics, 23*, 75–106.

Morrone, M. C., Burr, D. C., & Di Pietro, S. (1999). Cardinal directions for visual optic flow. *Current Biology, 9*(14), 763–766.

Morrone, M. C., Burr, D. C., & Vaina, L. M. (1995). 2 Stages of visual processing for radial and circular motion. *Nature, 376*(6540), 507–509.

Murakami, I., & Shimojo, S. (1993). Motion capture changes to induced motion at higher luminance contrasts, smaller eccentricities, and larger inducer sizes. *Vision Research, 33*, 2091–2107.

Nakayama, K., & Loomis, J. M. (1974). Optical velocity patterns, velocity-sensitive neurons, and space perception: A hypothesis. *Perception, 3*, 63–80.

Nakayama, K., & Tyler, C. W. (1981). Psychophysical isolation of movement sensitivity by removal of familiar position cues. *Vision Research, 21*(4), 427–433.

Nawrot, M., & Sekuler, R. (1990). Assimilation and contrast in motion perception—explorations in cooperativity. *Vision Research, 30*(10), 1439–1451.

Nazir, T. A. (1992). Effects of lateral masking and spatial precuing on gap- resolution in central and peripheral-vision. *Vision Research, 32*(4), 771–777.

Orban, G. A., Lagae, L., Raiguel, S., Xiao, D., & Maes, H. (1995). The speed tuning of medial superior temporal (MST) cell responses to optic-flow components. *Perception, 24*(3), 269–285.

Ortiz, A. (2001). Can letter-position uncertainty account for lateral masking? *Investigative Ophthalmology Visual Science, 42*(4), S4557.

Parkes, L., Lund, J., Angelucci, A., Solomon, J. A., & Morgan, M. (2001). Compulsory averaging of crowded orientation signals in human vision. *Nature Neuroscience, 4*(7), 739–744.

Pelli, D. G. (1997). The VideoToolbox software for visual psychophysics: Transforming numbers into movies. *Spatial Vision, 10*, 437–442.

Pelli, D. G., & Zhang, L. (1991). Accurate control of contrast on microcomputer displays. *Vision Research, 31*(7–8), 1337–1350.

Polat, U., & Sagi, D. (1993). Lateral interactions between spatial channels—suppression and facilitation revealed by lateral masking experiments. *Vision Research, 33*(7), 993–999.

Press, W. H., Teukolsky, A. A., Vetterling, W. T., & Flannery, B. P. (1992). *Numerical recipes in C*. Cambridge: Cambridge University Press.

Raiguel, S., Vanhulle, M. M., Xiao, D. K., Marcar, V. L., & Orban, G. A. (1995). Shape and spatial-distribution of receptive-fields and antagonistic motion surrounds in the middle temporal area (V5) of the macaque. *European Journal of Neuroscience, 7*(10), 2064–2082.

Regan, D., & Beverly, K. I. (1978). Looming detectors in the human visual pathway. *Vision Research, 18*, 415–421.

Regan, D., & Beverley, K. I. (1984). Figure-ground segregation by motion contrast and by luminance contrast. *Journal of Optical Society of America, 1*, 433–442.

Royden, C. S. (1997). Mathematical analysis of motion-opponent mechanisms used in the determination of heading and depth. *Journal of the Optical Society of America a—Optics Image Science and Vision, 14*(9), 2128–2143.

Royden, C. S. (2002). Computing heading in the presence of moving objects: A model that uses motion-opponent operators. *Vision Research, 42*(28), 3043–3058.

Sachtler, W. L., & Zaidi, Q. (1993). Effect of spatial configuration on motion aftereffects. *Journal of the Optical Society of America a—Optics Image Science and Vision, 10*(7), 1433–1449.

Sachtler, W. L., & Zaidi, Q. (1995). Visual processing of motion boundaries. *Vision Research, 35*(6), 807–826.

Saito, H., Tanaka, K., Isono, H., Yasuda, M., & Mikami, A. (1989). Directionally selective responses of cells in the middle temporal area (MT) of the macaque monkey to the movement of equiluminous opponent colour stimuli. *Experimental Brain Research, 75*, 1–14.

Schiller, P. H., Finlay, B. L., & Volman, S. F. (1976). Quantitative studies of single-cell properties in monkey striate cortex. I. Spatiotemporal organization of receptive fields. *Journal of Neurophysiology, 39*, 1288–1399.

Shioiri, S., Ito, S., Sakurai, K., & Yaguchi, H. (2002). Detection of relative and uniform motion. *Journal of the Optical Society of America a—Optics Image Science and Vision, 19*(11), 2169–2179.

Snowden, R. J., & Milne, A. B. (1996). The effects of adapting to complex motions: Position invariance and tuning to spiral motions. *Journal of Cognitive Neuroscience, 8*(5), 435–452.

Snowden, R. J., & Milne, A. B. (1997). Phantom motion aftereffects—evidence of detectors for the analysis of optic flow. *Current Biology, 7*, 717–722.

Strasburger, H., Harvey, L. O., & Rentschler, I. (1991). Contrast thresholds for identification of numeric characters in direct and eccentric view. *Perception and Psychophysics, 49*(6), 495–508.

Strelow, E. R., & Day, R. H. (1971). Aftereffect of visual movement: Storage in the absence of a patterned surround. *Perception and Psychophysics, 9*, 485–486.

Tanaka, K., & Saito, H. (1989). Analysis of motion of the visual field by direction, expansion/contraction, and rotation cells clustered in the dorsal part of the medial superior temporal area of the macaque monkey. *Journal of Neurophysiology, 62*, 626–641.

Toet, A., & Levi, D. M. (1992). The 2-dimensional shape of spatial interaction zones in the parafovea. *Vision Research, 32*(7), 1349–1357.

Townsend, J. T., Taylor, S. G., & Brown, D. R. (1971). Lateral masking for letters with unlimited viewing time. *Perception and Psychophysics, 10*, 375–378.

Treisman, A. (1987). Properties, parts and objects. In K. R. Boff, L. Kaufman, & F. P. Thomas (Eds.), *Handbook of perception and human performance*. New York: Wiley.

Tripathy, S. P., & Cavanagh, P. (2002). The extent of crowding in peripheral vision does not scale with target size. *Vision Research, 42*(20), 2357–2369.

Tripathy, S. P., & Levi, D. M. (1999). Looking behind a pathological blind spot in human retinal. *Vision Research, 39*(11), 1917–1925.

van Doorn, A. J., & Koenderink, J. J. (1982). Spatial properties of the visual detectability of moving spatial white noise. *Experimental Brain Research, 45*(1–2), 189–195.

Verghese, P., & Stone, L. S. (1995). Combining speed information across space. *Vision Research, 35*(20), 2811–2823.

Verghese, P., & Stone, L. S. (1996). Perceived visual speed constrained by image segmentation. *Nature, 381*(9/5/96), 161–163.

Watson, A. B., & Eckert, M. P. (1994). Motion-contrast sensitivity: Visibility of motion gradients of various spatial frequencies. *Journal of the Optical Society of America A, 11*, 496–505.

Watson, A. B., & Pelli, D. G. (1983). QUEST: A Bayesian adaptive psychometric method. *Perception and Psychophysics, 33*, 113–120.

Waugh, S. J., & Hess, R. F. (1994). Suprathreshold temporal-frequency discrimination in the fovea and the periphery. *Journal of Optical Society of America A, 11*, 1199–1212.

Wilkinson, F., James, T. W., Wilson, H. R., Gati, J. S., Menon, R. S., & Goodale, M. A. (2000). An fMRI study of the selective activation of human extrastriate form vision areas by radial and concentric gratings. *Current Biology, 10*(22), 1455–1458.

Wilkinson, F., Wilson, H. R., & Ellemberg, D. (1997). Lateral interactions in peripherally viewed texture arrays. *Journal of the Optical Society of America a—Optics Image Science and Vision, 14*(9), 2057–2068.

Wilson, H. R., McFarlane, D. K., & Phillips, G. C. (1983). Spatial frequency tuning of orientation selective units estimated by oblique masking. *Vision Research, 23*(9), 873–882.

Wilson, H. R., & Wilkinson, F. (1998). Detection of global structure in Glass patterns: Implications for form vision. *Vision Research, 38*(19), 2933–2947.

Wilson, H. R., Wilkinson, F., & Asaad, W. (1997). Concentric orientation summation in human form vision. *Vision Research, 37*(17), 2325–2330.

Wolford, G., & Chambers, L. (1984). Contour interaction as a function of eccentricity. *Perception and Psychophysics, 36*, 457–460.

Wright, M. J., & Johnston, A. (1983). Spatiotemporal contrast sensitivity and visual field locus. *Vision Research, 23*(10), 983–989.

Wurtz, R. H. (1969). Visual receptive fields of striate cortex neurons in awake monkeys. *Journal of Neurophysiology, 32*, 727–742.

Zenger, B., & Sagi, D. (1996). Isolating excitatory and inhibitory nonlinear spatial interactions involved in contrast detection. *Vision Research, 36*(16), 2497–2513.